Update on Cu_2OSeO_3:

Skyrmions in the 19th century, update on linear optical phenomena, and the cluster

Rolf B. Versteeg
Group meeting

27-06-18

Their connection? : Skyrmion

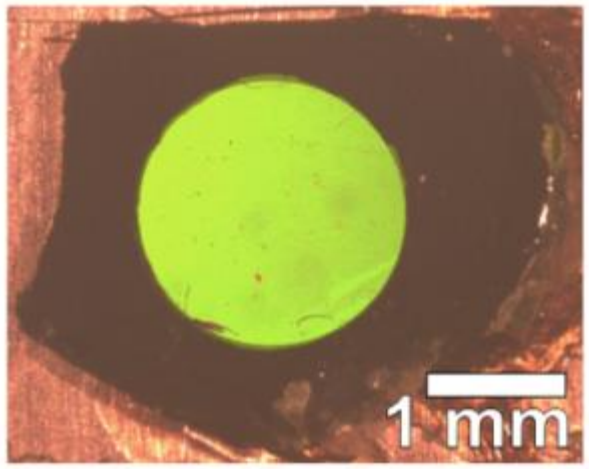

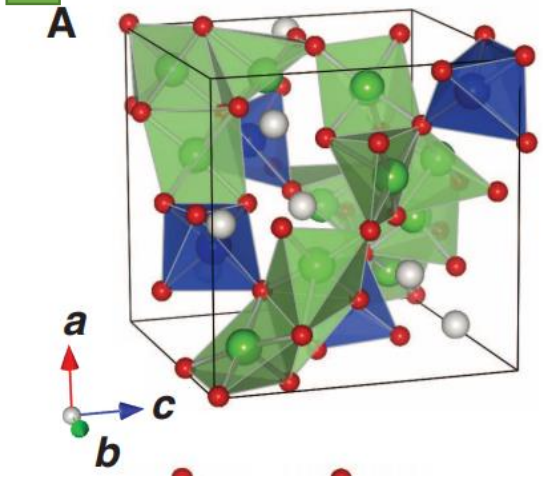

S. Seki, Science 336, 2012

Synthetic electromagnetic knot in a three-dimensional skyrmion

W. Lee et al., Sci. Adv. 2018;4: eaao3820

Wonjae Lee,[1]* Andrei H. Gheorghe,[1†] Konstantin Tiurev,[2] Tuomas Ollikainen,[2] Mikko Möttönen,[2,3] David S. Hall[1‡]

Classical electromagnetism and quantum mechanics are both central to the modern understanding of the physical world and its ongoing technological development. Quantum simulations of electromagnetic forces have the potential to provide information about materials and systems that do not have conveniently solvable theoretical descriptions, such as those related to quantum Hall physics, or that have not been physically observed, such as magnetic monopoles. However, quantum simulations that simultaneously implement all of the principal features of classical electromagnetism have thus far proved elusive. We experimentally realize a simulation in which a charged quantum particle interacts with the knotted electromagnetic fields peculiar to a topological model of ball lightning. These phenomena are induced by precise spatiotemporal control of the spin field of an atomic Bose-Einstein condensate, simultaneously creating a Shankar skyrmion—a topological excitation that was theoretically predicted four decades ago but never before observed experimentally. Our results reveal the versatile capabilities of synthetic electromagnetism and provide the first experimental images of topological three-dimensional skyrmions in a quantum system.

- Rubidium gas in magneto-optical trap
- Combination of normal magnetic fields, and quadrupole magnetic field (all a few Gauss)
- Create electromagnetic Skyrmion

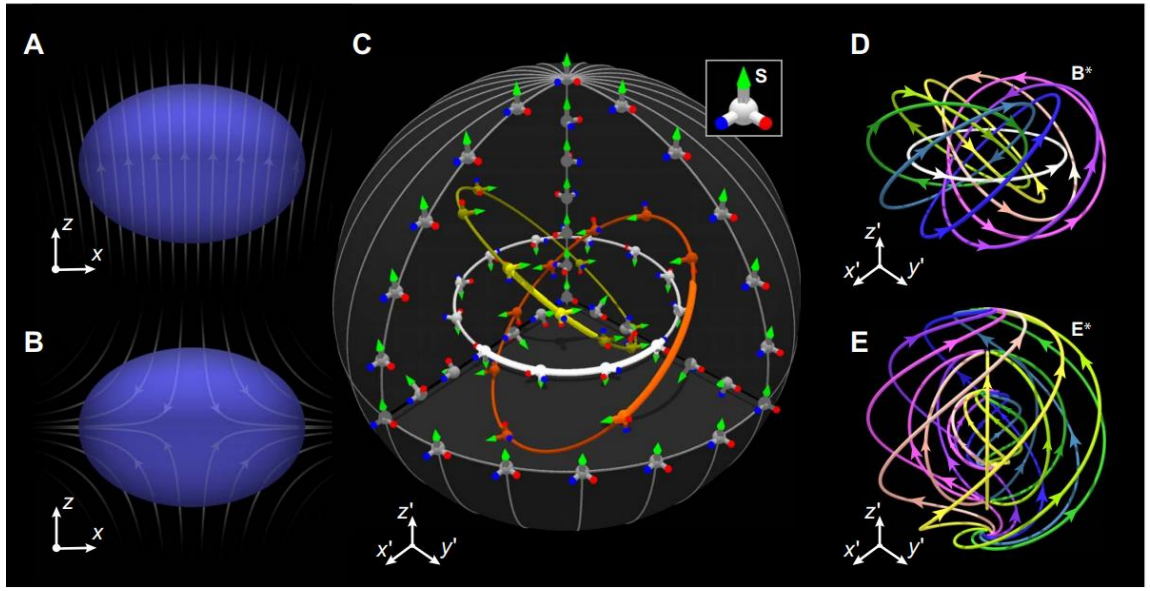

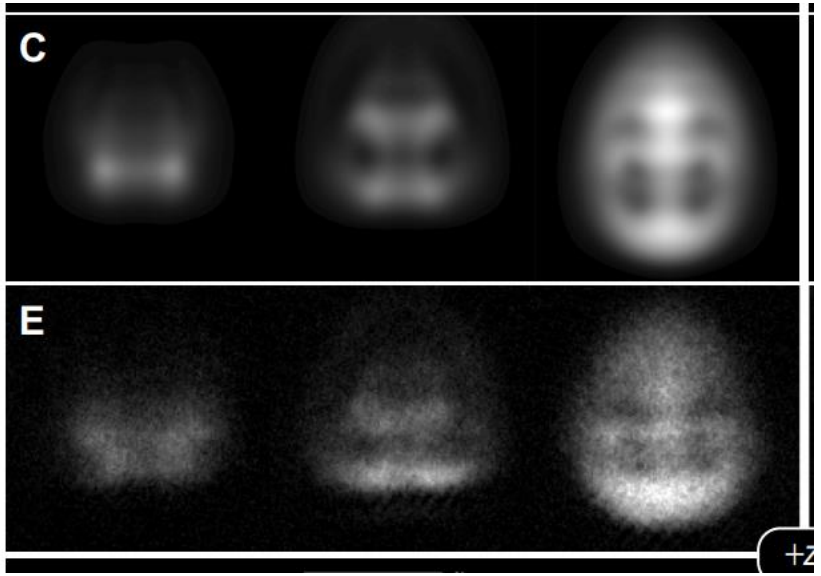

MagnetoChiral Dichroism in Cu_2OSeO_3

$$\nabla \times \mathbf{H} = \frac{1}{c}\frac{\partial \mathbf{D}}{\partial t} + \frac{\mathbf{j}}{c}$$

$$\nabla \times \mathbf{E} = -\frac{1}{c}\frac{\partial \mathbf{B}}{\partial t}$$

$$\nabla \cdot \mathbf{D} = \rho$$

$$\nabla \cdot \mathbf{B} = 0$$

Maxwell equations

+

$$\mathbf{D} = \epsilon \mathbf{E}$$

$$\mathbf{B} = \mu \mathbf{H}$$

$$\mathbf{j} = \sigma \mathbf{E}$$

Constitutive equations

=

Crystal symmetry

Propagation mode polarization

$$\sum_j (\epsilon_{ihj} + s_i s_j) E_j = n^2 I E_i$$

Wave vector K

$$\mathbf{k} = \frac{\omega n}{c}\hat{\mathbf{s}}$$

Propagation in matter:
±**k**, both have 2 transversal orthogonal polarizations

The dielectric permittivity tensor for a chiral magnetized material thus takes the form $\boldsymbol{\epsilon}(\omega,\mathbf{k},\mathbf{M})$. [9] The effects of spatial dispersion and magnetization, can be taken into account by expanding $\boldsymbol{\epsilon}$ in first and second order terms [4, 8, 9] of $\mathbf{k}$ and $\mathbf{M}$. This is most easily done in the Einstein summation notation:

$$\epsilon_{ij} = \epsilon^0_{ij} + i\gamma_{ijl}k_l + \alpha_{ijlm}k_l k_m + f_{ijn}M_n + g_{ijnp}M_n M_p + \eta_{ijln}k_l M_n \qquad (27)$$

Faraday, Natural Optical Activity observed: $\theta_T + i\eta_T = \frac{\omega d}{2c} \frac{i\epsilon_{xy}}{\sqrt{\epsilon_{xx}}}$

The magnetic chiral structure allows for an additional higher-order optical effect, namely, nonreciprocal directional dichroism [13,14]. In Cu_2OSeO_3 this effect has been observed for microwave resonance modes [55]. We have investigated this effect in the optical range (around 2.3 eV) for the various magnetic phases at 15 K, but have not been able to make a conclusive observation. Given the sensitivity of our setup, this limits a possible nonreciprocal directional dichroism to well below 1%.

Optically probed paper, PRB94 (2016)

Table 1: Overview of optical anisotropies in a chiral magnet: An anisotropy can be observed when the indicated operations for inversion i, time-reversal t, and the combined operation $i \cdot t$ aren't $(-)$ a symmetry of the material anymore. The operation indicated with $(+)$ may still be a valid symmetry operation to observe the respective optical phenomenon. The last column indicates from which dielectric tensor expansion term the optical effect originates.

crystal optics phenomenon	i	t	i and t	$i \cdot t$	expansion term
linear birefringence and dichroism	+	+	+	+	ϵ_{ij}^0
natural circular birefringence and dichroism	−	+	−	−	$i\gamma_{ijl}k_l$
second-order spatial birefringence and dichroism	+	+	+	+	$\alpha_{ijlm}k_l k_m$
magnetic circular birefringence and dichroism	+	−	−	−	$f_{ijn}M_n$
magnetic linear birefringence and dichroism	+	−	−	−	$g_{ijnp}M_n M_p$
gyrotropic birefringence and dichroism	−	−	−	+	$i\gamma_{ijl}k_l$
magnetochiral birefringence and dichroism	−	−	−	−	$\eta_{ijln}k_l M_n$
optical magnetoelectric birefringence and dichroism	−	−	−	−	$\phi_{ijlnq}k_l M_n P_q$

A fun-fact from this literature search:

- Materials such as Silicon and CaF_2 are in fact optically anistropic! ~k^2 higher order natural optical activity.

Nonreciprocal dichroism

- Difference between **+k** and **–k** direction: **revert time**
- Q: What does reverting time do?
  - **+k → -k**
  - Magnetic field reverses: **+B→ -B**
  - Photon helicity **stays the same** (in photon reference frame)

- Q: Is Natural Optical Activity “nonreciprocal”?:
- A: **NO**: in time-inverted experiment the L-handed crystal still sees same helicity of photon.

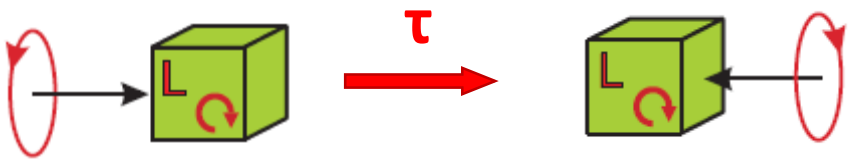

- Q: Is Magnetic Circular Dichroism/Faraday/Kerr “nonreciprocal”?
- **YES**: in time-inverted experiment the circularly polarized light sees another crystal. “not physical: crystal stays the same”

- Conclusion: Faraday effect (broken T-symmetry) distinguishes between propagation direction for circularly polarized light!: Nonreciprocal dichroism for **circular light!!**

The dielectric permittivity tensor for a chiral magnetized material thus takes the form $\boldsymbol{\epsilon}(\omega,\mathbf{k},\mathbf{M})$. [9] The effects of spatial dispersion and magnetization, can be taken into account by expanding $\boldsymbol{\epsilon}$ in first and second order terms [4, 8, 9] of $\mathbf{k}$ and $\mathbf{M}$. This is most easily done in the Einstein summation notation:

$$\epsilon_{ij} = \epsilon^0_{ij} + i\gamma_{ijl}k_l + \alpha_{ijlm}k_l k_m + f_{ijn}M_n + g_{ijnp}M_n M_p + \eta_{ijln}k_l M_n$$

$$\epsilon_{ij} = \begin{pmatrix} \epsilon_{xx} + \mathbf{k}\cdot\mathbf{M} & f\mathbf{M} & 0 \\ -f\mathbf{M} & \epsilon_{xx} + \mathbf{k}\cdot\mathbf{M} & 0 \\ 0 & 0 & \epsilon_{xx} \end{pmatrix}$$

k·M term on diagonal: different absorption for ± **k** direction! (also on diagonal): **nonreciprocal**

Data from Geert Rikken, Toulouse, France

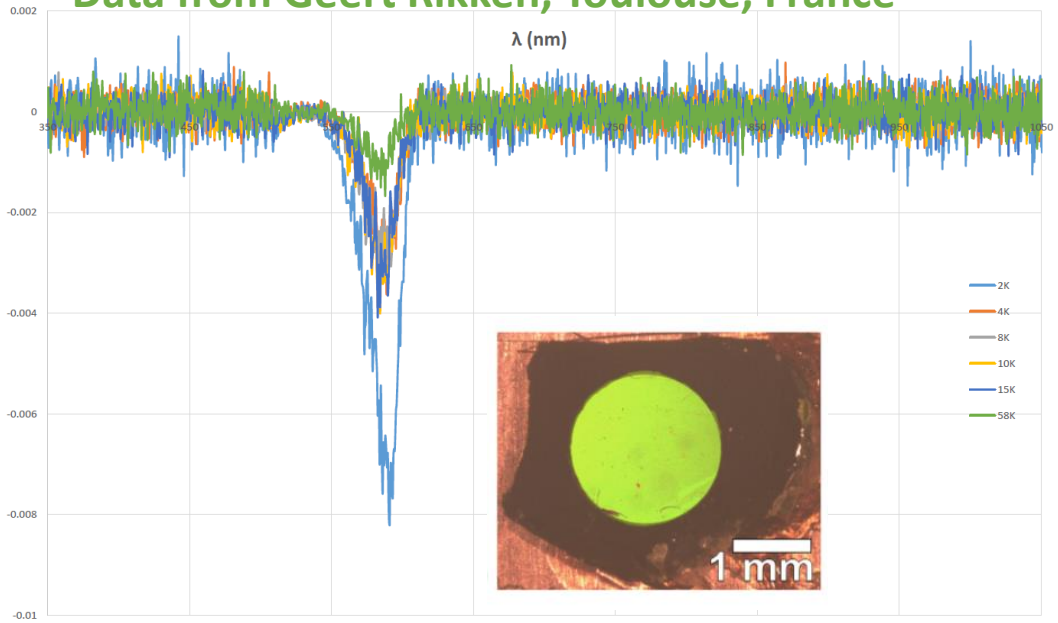

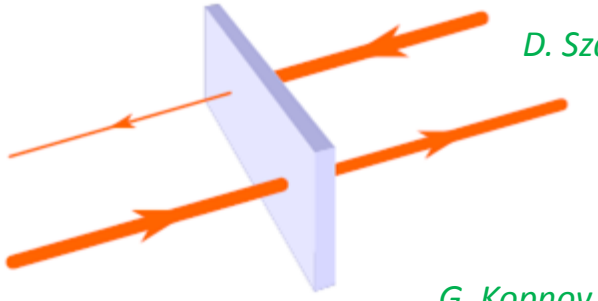

D. Szaller, PRB 87 (2013)

G. Kopnov, Rev Sci Instrum 85 (2014)

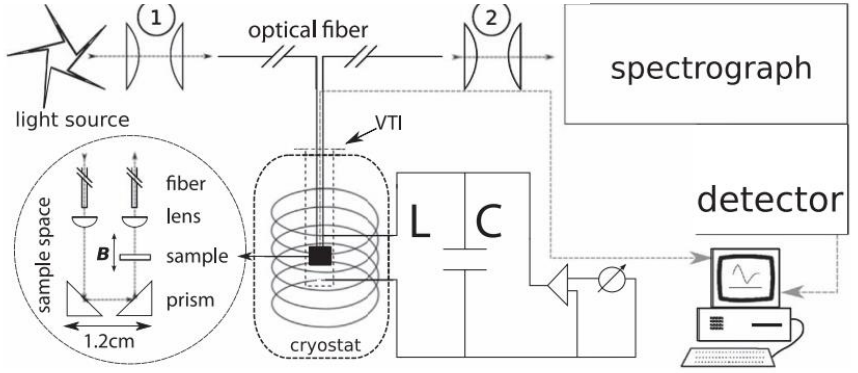

The dielectric permittivity tensor for a chiral magnetized material thus takes the form $\boldsymbol{\epsilon}(\omega,\mathbf{k},\mathbf{M})$. [9] The effects of spatial dispersion and magnetization, can be taken into account by expanding $\boldsymbol{\epsilon}$ in first and second order terms [4, 8, 9] of $\mathbf{k}$ and $\mathbf{M}$. This is most easily done in the Einstein summation notation:

$$\epsilon_{ij} = \epsilon^0_{ij} + i\gamma_{ijl}k_l + \alpha_{ijlm}k_l k_m + f_{ijn}M_n + g_{ijnp}M_n M_p + \eta_{ijln}k_l M_n \tag{27}$$

Table 1: Overview of optical anisotropies in a chiral magnet: An anisotropy can be observed when the indicated operations for inversion i, time-reversal t, and the combined operation $i \cdot t$ aren't $(-)$ a symmetry of the material anymore. The operation indicated with $(+)$ may still be a valid symmetry operation to observe the respective optical phenomenon. The last column indicates from which dielectric tensor expansion term the optical effect originates.

crystal optics phenomenon	i	t	i and t	$i \cdot t$	expansion term
linear birefringence and dichroism	$+$	$+$	$+$	$+$	ϵ^0_{ij}
natural circular birefringence and dichroism	$-$	$+$	$-$	$-$	$i\gamma_{ijl}k_l$
second-order spatial birefringence and dichroism	$+$	$+$	$+$	$+$	$\alpha_{ijlm}k_l k_m$
magnetic circular birefringence and dichroism	$+$	$-$	$-$	$-$	$f_{ijn}M_n$
magnetic linear birefringence and dichroism	$+$	$-$	$-$	$-$	$g_{ijnp}M_n M_p$
gyrotropic birefringence and dichroism	$-$	$-$	$-$	$+$	$i\gamma_{ijl}k_l$
magnetochiral birefringence and dichroism	$-$	$-$	$-$	$-$	$\eta_{ijln}k_l M_n$
optical magnetoelectric birefringence and dichroism	$-$	$-$	$-$	$-$	$\phi_{ijlnq}k_l M_n P_q$

Cu_4 spin cluster understanding

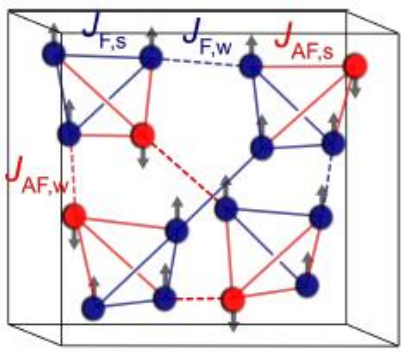

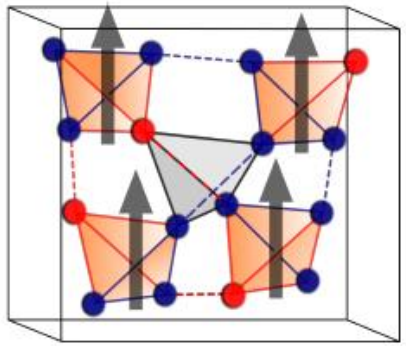

Table 1: Isolated single cluster states and eigenenergies. In total there are 16 states for the isolated cluster. The states are indicated in the full notation $|S_{23}, S_{234}, S, S^z\rangle_{\mathrm{R}}$, the shortened notation $|S, S^z\rangle_{\mathrm{R}}$, and indicated are the degeneracies D. E_n gives the energy of the degenerate states. $\Delta\mathrm{E}_n$ gives the energy measured with respect to the ground state energy E_0. The last two columns give the calculated transition energies in wavenumbers cm^{-1} and temperature K.

n	$\lvert S_{23}, S_{234}, S, S^z\rangle_{\mathrm{R}}$	$\lvert S, S^z\rangle_{\mathrm{R}}$	D	E_n	$\Delta\mathrm{E}_n = \mathrm{E}_n - E_0$	$\Delta\mathrm{E}_n(\mathrm{cm}^{-1})$	$\Delta\mathrm{E}_n(\mathrm{K})$
0	$\lvert 1, \frac{3}{2}, 1, S^z\rangle_{\mathrm{A}_1}$	$\lvert 1, S^z\rangle_{\mathrm{A}_1}$	3	$\frac{1}{4}(-5J_{\mathrm{AF,s}} + 3J_{\mathrm{FM,s}})$	0	0	0
1	$\lvert 1, \frac{1}{2}, 0, S^z\rangle_{\mathrm{E}_1}$	$\lvert 0, S^z\rangle_{\mathrm{E}_1}$	1	$-\frac{3}{4}(J_{\mathrm{AF,s}} + J_{\mathrm{FM,s}})$	$\frac{1}{2}(J_{\mathrm{AF,s}} - 3J_{\mathrm{FM,s}})$	191	275
	$\lvert 0, \frac{1}{2}, 0, S^z\rangle_{\mathrm{E}_2}$	$\lvert 0, S^z\rangle_{\mathrm{E}_2}$	1				
2	$\lvert 1, \frac{3}{2}, 2, S^z\rangle_{\mathrm{A}_1}$	$\lvert 2, S^z\rangle_{\mathrm{A}_1}$	5	$\frac{3}{4}(J_{\mathrm{AF,s}} + J_{\mathrm{FM,s}})$	$2J_{\mathrm{AF,s}}$	236	340
3	$\lvert 1, \frac{1}{2}, 1, S^z\rangle_{\mathrm{E}_1}$	$\lvert 1, S^z\rangle_{\mathrm{E}_1}$	3	$\frac{1}{4}(J_{\mathrm{AF,s}} - 3J_{\mathrm{FM,s}})$	$\frac{3}{2}(J_{\mathrm{AF,s}} - J_{\mathrm{FM,s}})$	309	445
	$\lvert 0, \frac{1}{2}, 1, S^z\rangle_{\mathrm{E}_2}$	$\lvert 1, S^z\rangle_{\mathrm{E}_2}$	3				

$$\mathcal{H}_0 = J_s^{\mathrm{AF}}\mathbf{S}_1 \cdot \mathbf{S}_{234} + J_s^{\mathrm{FM}}(\mathbf{S}_2 \cdot \mathbf{S}_3 + \mathbf{S}_3 \cdot \mathbf{S}_4 + \mathbf{S}_4 \cdot \mathbf{S}_2)$$
$$= \frac{J_s^{\mathrm{AF}}}{2}\mathbf{S}^2 + \frac{J_s^{\mathrm{FM}} - J_s^{\mathrm{AF}}}{2}\mathbf{S}_{234}^2 - \frac{3}{8}(J_s^{\mathrm{AF}} + 3J_s^{\mathrm{FM}})$$

The expectation values for the angular momentum operators are:

$$\mathbf{S}^2|S_{23}, S_{234}, S, S^z\rangle = S(S+1)|S_{23}, S_{234}, S, S^z\rangle$$

and

$$\mathbf{S}_{234}^2|S_{23}, S_{234}, S, S^z\rangle = S_{234}(S_{234}+1)|S_{23}, S_{234}, S, S^z\rangle$$

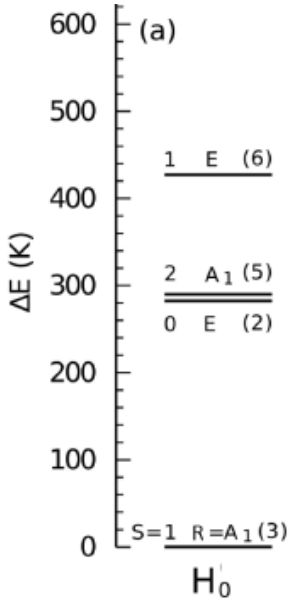

J. Romhanyi et al. PRB 90 (2014)

Isolated Cu4 cluster spectrum

J. Romhanyi et al. PRB 90 (2014)

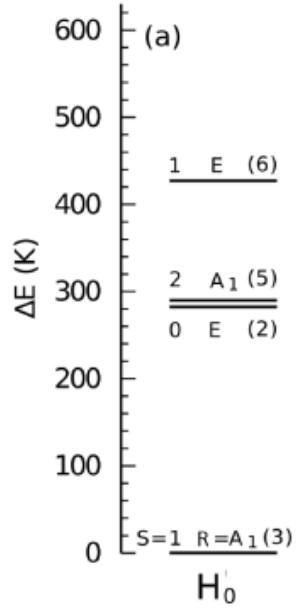

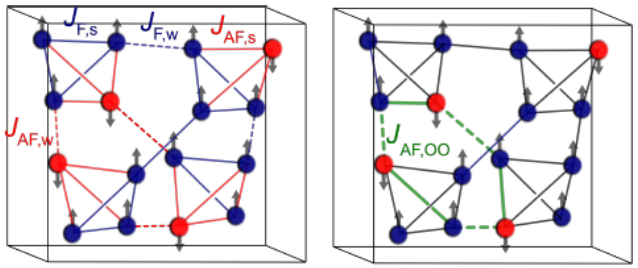

Cu4 cluster in mean-field

J. Romhanyi et al. PRB 90 (2014)

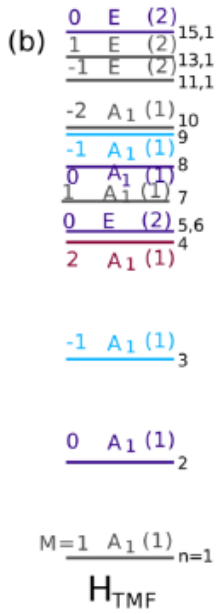

$$\mathcal{H}_{\mathrm{TMF}} = \mathcal{H}_0 + J_{\mathrm{AF,s}}(\delta S_1^z + \Delta S_{234}^z)$$

$$\delta = 3\langle S_1^z\rangle(J_{\mathrm{AF,w}} + J_{\mathrm{AF,OO}})/J_{\mathrm{AF,s}} > 0$$

$$\Delta = \left[\langle S_1^z\rangle(J_{\mathrm{AF,w}} + J_{\mathrm{AF,OO}}) + 2\langle S_2^z\rangle J_{\mathrm{F,w}}\right]/J_{\mathrm{AF,s}} < 0$$

Cu4 cluster in mean-field + 2nd quantization

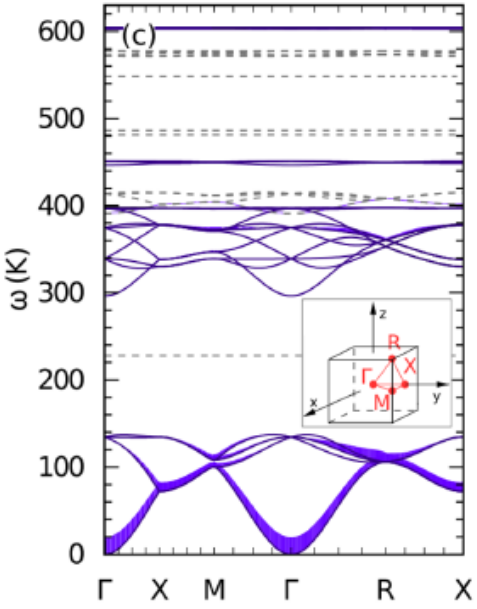

J. Romhanyi et al. PRB 90 (2014)

$$\sum_n a_{n,\nu}^{\dagger}(\mathbf{R})a_{n,\nu}(\mathbf{R}) = 1.$$

TABLE I. The eigenspectrum of $\mathcal{H}_0^{(t)}$ and $\mathcal{H}_{\mathsf{TMF}}^{(t)}$, classified in terms of the total spin projection M along the quantization axis and the symmetry sectors λ of the point group C_{3v}, see text. The symbol j_f stands for the ratio $j_f = J_s^{\mathsf{FM}}/J_s^{\mathsf{AF}}$.

n	λ	M	$(E_0 - E_{GS})/J_s^{\mathsf{AF}}$	$(E_{\mathsf{TMF}} - E_{GS})/J_s^{\mathsf{AF}}$
1	A_1	1		$1+\Delta-[1+\frac{\delta-\Delta}{2}+(\frac{\delta-\Delta}{2})^2]^{1/2} \simeq \frac{-\delta+5\Delta}{4}$
2	A_1	0	0	$1-[1+(\frac{\delta-\Delta}{2})^2]^{1/2} \simeq 0$
3	A_1	−1		$1-\Delta-[1+\frac{\delta-\Delta}{2}+(\frac{\delta-\Delta}{2})^2]^{1/2} \simeq -\frac{\delta+3\Delta}{4}$
4 5	E	0	$\frac{1}{2}(1-3j_f)$	$1-\frac{3}{2}j_f-\frac{1}{2}[1+(\delta-\Delta)^2]^{1/2} \simeq \frac{1-3j_f}{2}$
6	A_1	−2		$2-\frac{\delta+3\Delta}{2}$
7	A_1	−1		$1-\Delta+[1+\frac{\delta-\Delta}{2}+(\frac{\delta-\Delta}{2})^2]^{1/2} \simeq 2+\frac{\delta-5\Delta}{4}$
8	A_1	0	2	$1+[1+(\frac{\delta-\Delta}{2})^2]^{1/2} \simeq 2$
9	A_1	1		$1+\Delta+[1+\frac{\delta-\Delta}{2}+(\frac{\delta-\Delta}{2})^2]^{1/2} \simeq 2+\frac{\delta+3\Delta}{4}$
10	A_1	2		$2+\frac{\delta+3\Delta}{2}$
11 12	E	−1		$\frac{3}{2}(1-j_f)-\frac{\delta+\Delta}{2}$
13 14	E	0	$\frac{3}{2}(1-j_f)$	$1-\frac{3}{2}j_f+\frac{\sqrt{1+(\delta-\Delta)^2}}{2} \simeq \frac{3}{2}(1-j_f)$
15 16	E	1		$\frac{3}{2}(1-j_f)+\frac{\delta+\Delta}{2}$

Cu4 cluster in mean field: Γ-point excitations with electron spin resonance (ESR)

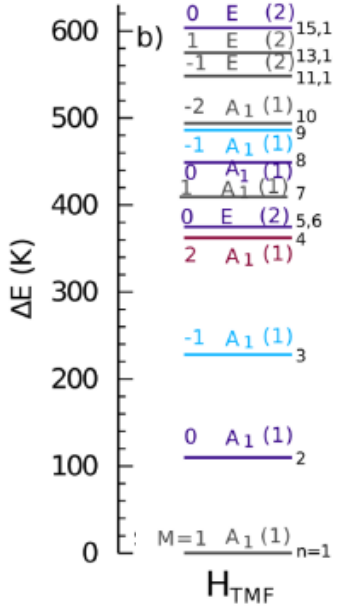

J. Romhanyi et al. PRB 90 (2014)

Ozerov et al. PRL 113 (2014)

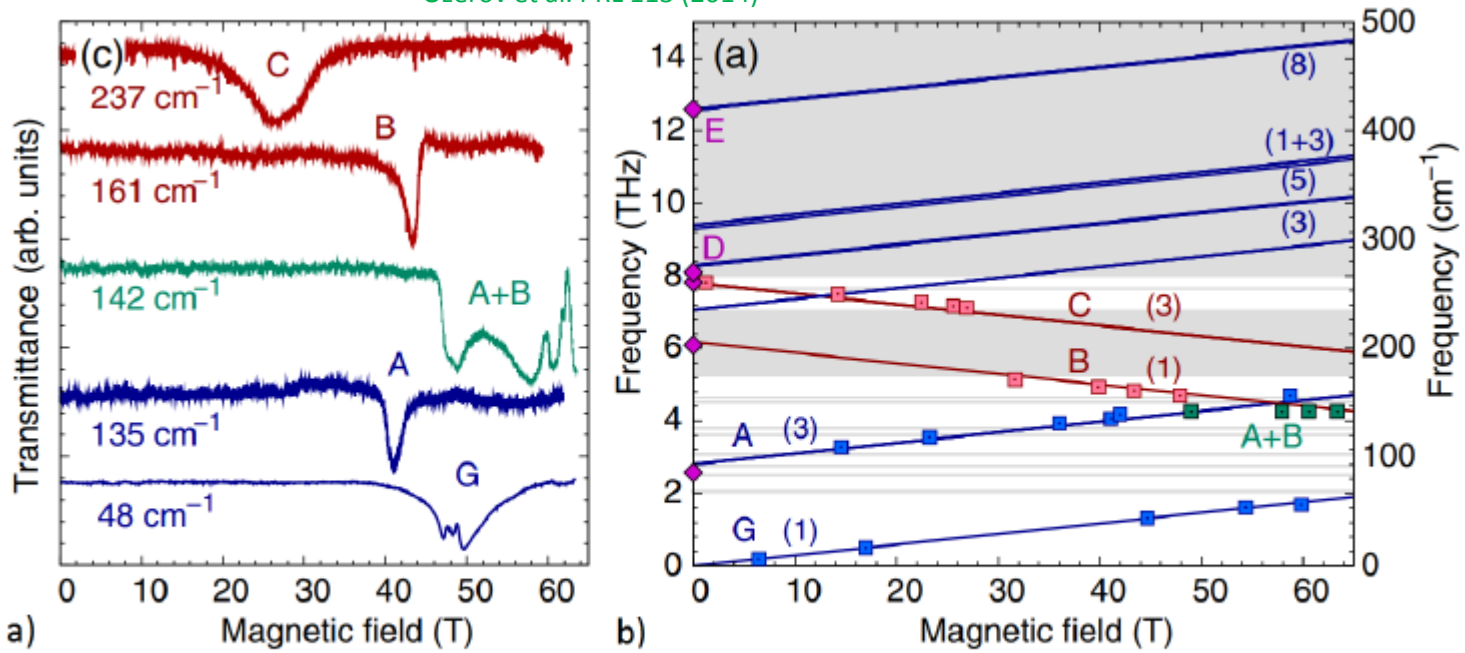

Figure 3: a) Figure adapted from Ref. [2]

Cu4 cluster in mean-field + 2nd quantization

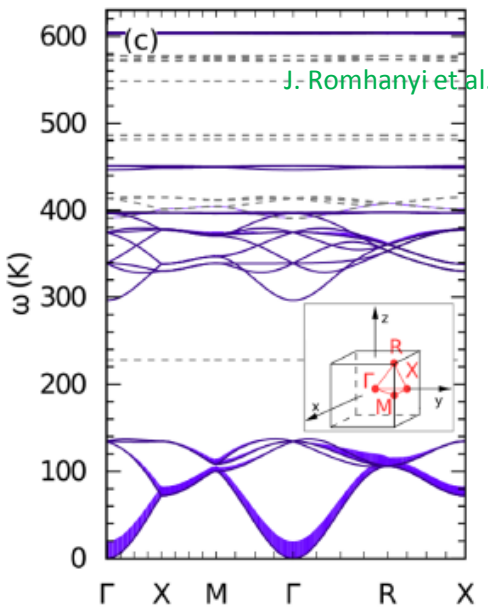

J. Romhanyi et al. PRB 90 (2014)

Cu_4 cluster including k-dependence: inelastic neutron spectrum

PY Portnichenko et al. Nat. Comm 7 (2016)

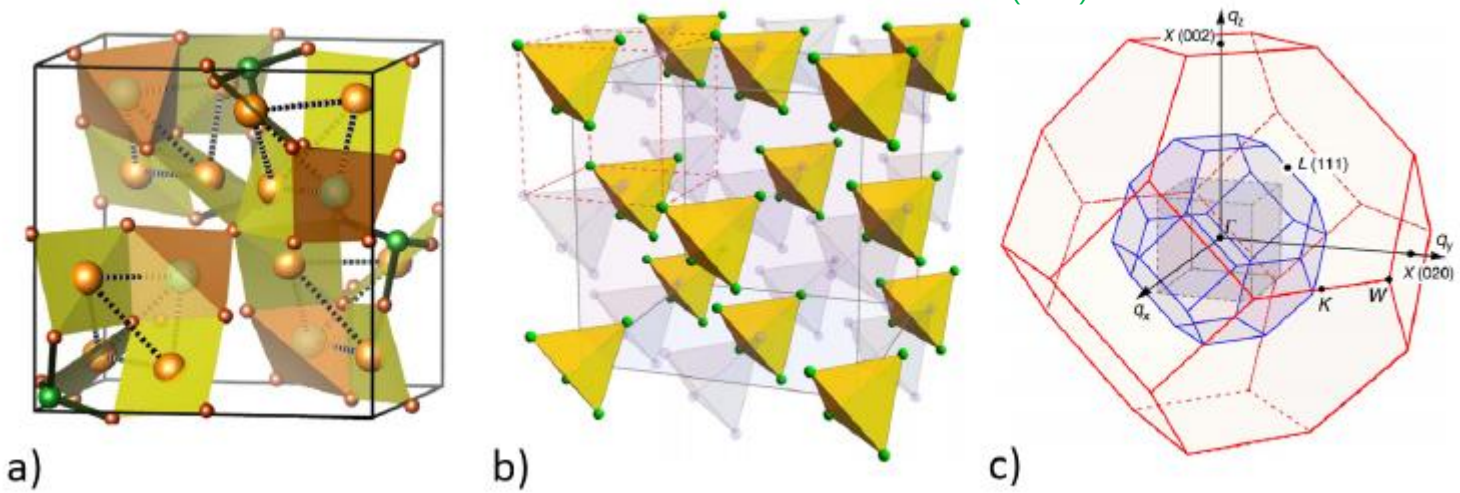

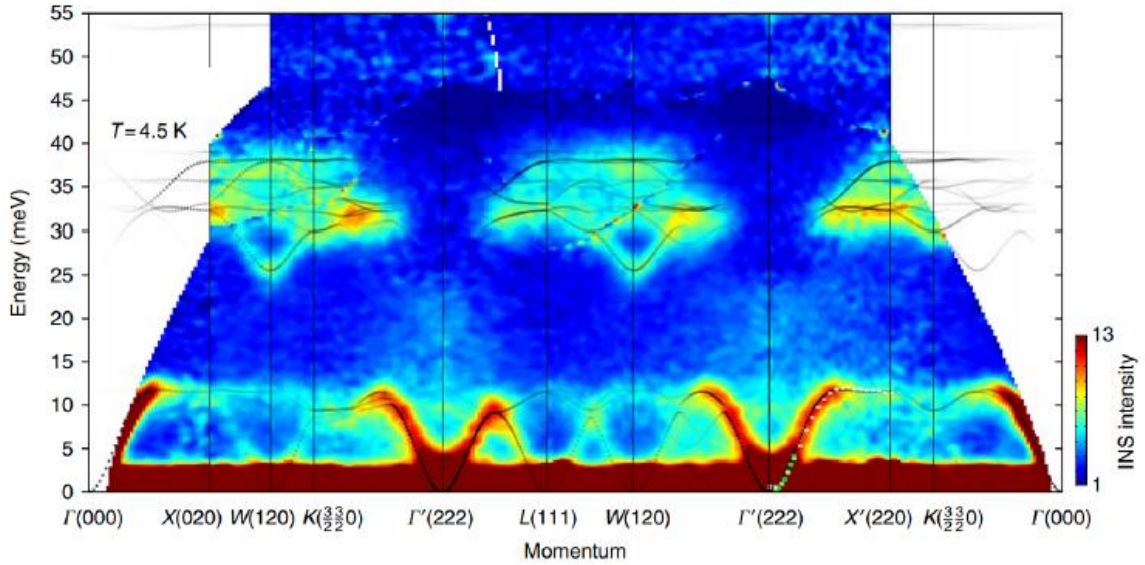

PY Portnichenko et al. Nat. Comm 7 (2016)

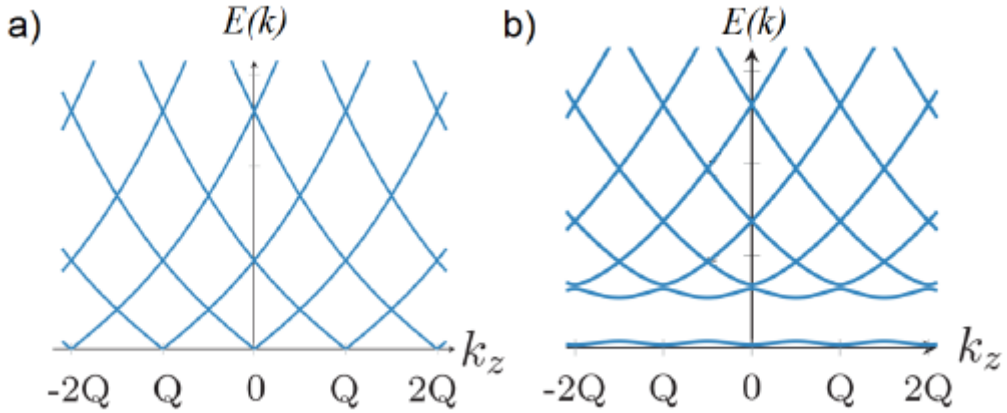

Markus Garst et al 2017 J. Phys. D: Appl. Phys. 50 293002

- Helimagnon bands in MnSi observed up to n=6 with inelastic neutron (M. Kugler et al. PRL115, 2015)

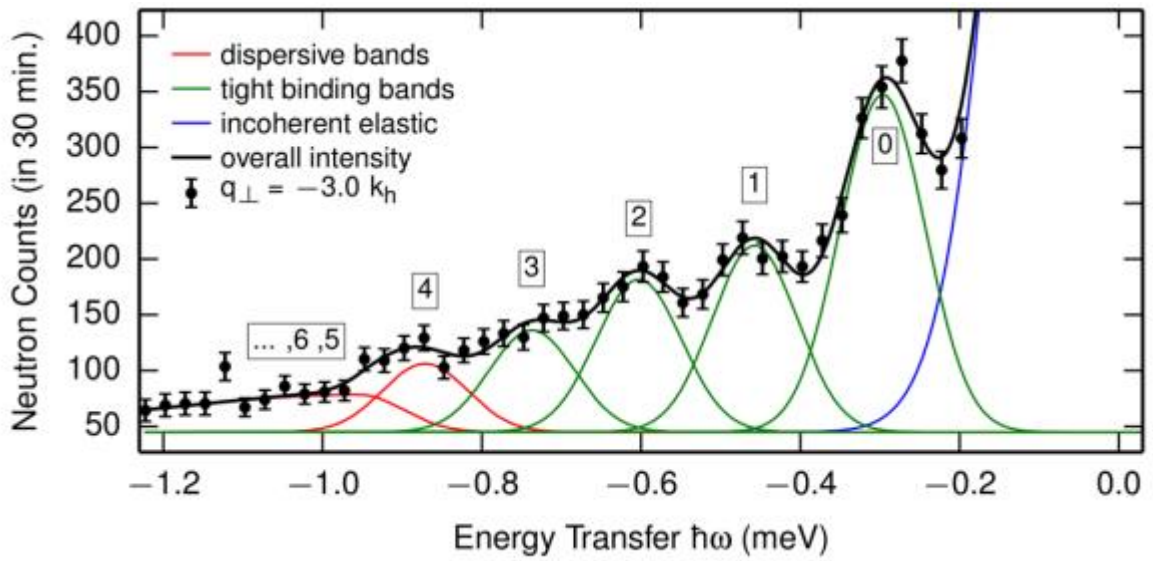

- Helimagnon bands in Cu_2OSeO_3 only up to n=3 observed by GHz-spectroscopy (M. Weiler et al. PRL119, 2017)
- Interesting task for Brillouin Scattering in magnetic field?